J Pharmacol Sci **104**, 61 – 72 (2007)

Journal of Pharmacological Sciences

Full Paper

Desipramine Activated Bcl-2 Expression and Inhibited Lipopolysaccharide-Induced Apoptosis in Hippocampus-Derived Adult Neural Stem Cells

Yu-Yin Huang[1,4,6,†], Chi-Hsien Peng[2,6,7,†], Yi-Ping Yang[3], Chih-Chiau Wu[2], Wen-Ming Hsu[2], Hsiao-Jung Wang[3], Kwok-Han Chan[1], Yi-Pen Chou[4], Shih-Jen Chen[2], and Yuh-Lih Chang[3,5,*]

[1]*Department of Anesthesiology,* [2]*Department of Ophthalmology,* [3]*Department of Pharmacy, Taipei Veterans General Hospital and National Yang-Ming University, Taipei, Taiwan*
[4]*Department of Anesthesiology, Cheng-Hsin Rehabilitation Medical Center, Taipei, Taiwan*
[5]*Department of Pharmacy, Chia Nan University of Pharmacy and Science, Tainan, Taiwan*
[6]*Institute of Clinical Medicine, National Yang-Ming University, Taipei, Taiwan*
[7]*Shin Kong Wu Ho-Su Memorial Hospital, Taipei, Taiwan*

Received October10, 2006; Accepted March 20, 2007

Abstract. Desipramine (DP) is a tricyclic antidepressant used for treating depression and numerous other psychiatric disorders. Recent studies have shown that DP can promote neurogenesis and improve the survival rate of hippocampal neurons. However, whether DP induces neuroprotection or promotes the differentiation of neural stem cells (NSCs) needs to be elucidated. In this study, we cultured NSCs derived from the hippocampal tissues of adult rats as an in vitro model to evaluate the modulation effect of DP on NSCs. First, we demonstrated that the expression of Bcl-2 mRNA and nestin in 2 μM DP-treated NSCs were up-regulated and detected by real-time reverse transcriptase polymerase chain reaction (RT-PCR). The results of Western blotting and immunofluorescent study confirmed that Bcl-2 protein expression was significantly increased in Day 3 DP-treated NSCs. Using the Bcl-2 small interfering RNA (siRNA) method, our results further showed that DP protects the lipopolysaccharide (LPS)-induced apoptosis in NSCs, in part by activating the expression of Bcl-2. Furthermore, DP treatment significantly inhibited the induction of proinflammatory factor interleukin (IL)-1β, IL-6, and tumor necrosis factor-α in the culture medium of LPS-treated NSCs mediated by Bcl-2 modulation. The results of high performance liquid chromatography coupled to electrochemical detection further confirmed that DP significantly increased the functional production of serotonin (26 ± 3.5 μM, DP-treated 96 h) and noradrenaline (50 ± 8.9 μM, DP-treated 96 h) in NSCs through activation of the MAPK/ERK pathway and partially mediated by Bcl-2. In conclusion, the present results indicate that DP can increase neuroprotection ability by inhibiting the LPS-induced inflammatory process in NSCs via the modulation of Bcl-2 expression, as confirmed by the siRNA method.

Keywords: desipramine, neural stem cell, real-time RT-PCR, small interfering RNA (siRNA)

Introduction

Desipramine (DP) is a tricyclic antidepressant that has been introduced as an effective drug to treat depressive mood disorders (1). It has been proved to be safe and effective for the treatment of depression as well as other psychiatric and neurodegenerative diseases (2). The previous study showed that DP exerts various in vitro and in vivo effects. Chronic DP treatment increases the membrane expression of AMPA receptors in rat hippocampus (3). Acute treatment with DP was shown to

[†]These authors contributed equally to this work.
*Correspondence author (affiliation #3). ylchang@vghtpe.gov.tw
Published online in J-STAGE
doi: 10.1254/jphs.FP0061255

inhibit SK3 channels in human medulloblastoma cells (4). DP also enhances glucocorticoid receptor function by modulating the membrane steroid transporters (5), and suppresses human cytochrome P450 enzymes and rat protein kinase C (6, 7).

Recently, pre-clinical and clinical findings have shown that hippocampal volume in patients with depression is reduced in comparison to the volume in healthy people (8). Clinical survey and magnetic resonance imaging (MRI) studies also showed that the hippocampal volume decreases in patients with depression and post-traumatic stress disorder (8, 9). Further studies have demonstrated that increased neurogenesis in the hippocampus by the administration of antidepressant drugs can result in altered behavior in stress-induced models and patients (10, 11). More recently, Chen et al. reported evidence that DP can promote neurogenesis in the hippocampus and reverse the learned behavior in learned helplessness rats (12). However, whether DP can promote neuroprotection and differentiation ability in the hippocampus in the central nervous system (CNS) has not been determined.

Neural stem cells (NSCs), derived from the hippocampus and other germinal centers of the brain, have been isolated and defined as cells with the capacity of self-renewal and multi-lineage differentiation (13 – 15). NSCs possess the utilizing potential to develop transplantation strategies and to screen the candidate agents for neurogenesis in neurodegenerative diseases (14). In order to elucidate the role of DP in neural progenitor proliferation, we cultured NSCs derived from the hippocampal tissues of adult rats as a model for the in vitro drug-effect test (16) and found that 2 μM DP can up-regulate Bcl-2 expression in DP-treated NSCs. In addition, previous studies have shown that major depression is accompanied by activation of the inflammatory-response system (17 – 19). In an experimental study on healthy young men, immune activation by administering endotoxin produced alternations in emotional states and an increase of reported depressive symptoms (20).

To further investigate whether DP inhibits the inflammatory process of NSCs or induces a neuroprotection effect in NSCs, the proinflammatory cytokines and apoptotic markers were monitored by ELISA and TUNEL assays in DP-pretreated NSCs with or without lipopolysaccharide (LPS) treatment. Furthermore, Bcl-2, an anti-apoptotic gene, is a target for the actions of mood stabilizers and mediates many of the beneficial effects of endogenous neurotrophic factors (21, 22). Hence, by using Bcl-2 gene silencing with small interfering RNA (siRNA), we aim to investigate the biological effects, neural proliferation, neuroprotection, and differentiation capability of DP on NSCs and to explore the associated mechanisms.

Materials and Methods

Isolation and culture of NSCs

All animals used were treated in accordance with the Animal Care and Use Committee guidelines at Taipei Veterans General Hospital. The protocol of the present study was also approved by the Committee. Adult Sprague-Dawley (SD) rats (8-week-old, 250 g) were anesthetized with intraperitoneal phenobarbital (Sigma Chemical Co., St. Louis, MO, USA) and the location of their brains was mapped. Then, the brain was surgically separated from the hippocampus region with the procedure described by Liu et al. (16). In brief, tissues from the hippocampus of adult rats were dissociated and incubated in Hank's balanced salt solution (HBSS) containing collagenase (78 units/mL) and hyaluronidase (38 units/mL) for 10 min at 37°C. The tissues were then mechanically dissected and placed in a trypsin solution (1.33 mg/mL) at 37°C for another 10 min. Dissociated cells were then centrifuged at 150 GG for 5 min. Then the enzyme solution was removed and replaced with serum-free culture media composed of Dulbecco's modified Eagle medium (DMEM) and F-12 nutrient mixture (1:1) including insulin (25 μg/mL), transferrin (100 μg/mL), progesterone (20 nM), putrescine (60 μM), sodium selenite (30 nM), human recombinant epidermal growth factor (EGF) (20 ng/mL), and fibroblast growth factor-basic (bFGF) (20 ng/mL) (R&D Systems, Minneapolis, MN, USA). Viable cells were counted by trypan blue exclusion and plated as 5000 cells/200 μL per well in 96-well plates (Corning, Inc., Acton, MA, USA) with no substrate pretreatment. The DP was purchased from Sigma Chem. Co. The vehicle control used in all procedures and studies was 0.1% dimethyl sulfoxide (DMSO) (Sigma Chem. Co.) Regarding the differentiation protocol, the neurosphere-like NSCs were plated on poly-L-ornithine–coated (15 μg/mL) glass coverslips in individual wells of 24-well plates (1.0 mL/well) in the DMEM/F-12 medium containing 2% fetal calf serum (FCS) (Gibco-BRL, Gaitherburg, MD, USA) and withdrawing EGF and bFGF. At the time of NSC seeding, the vehicle control or DP was concurrently added.

Cell viability assay and enzyme-linked immunosorbent assay (ELISA)

NSCs were seeded on 24-well plates at a density of 2×10^4 cells/well in medium, followed by the methyl thiazol tetrazolium assay (MTT assay) (Sigma-Aldrich Co., St. Louis, MO, USA) for determination of cell viability. NSCs were incubated with 0.25 mg/mL MTT

for 4 h at 37°C and the reaction was terminated by the addition of 100% isopropanol. The amount of MTT formazan product was determined by using a microplate reader and the absorbance was measured at 560 nm (SpectraMax 250; Molecular Devices, Sunnyvale, CA, USA). NSCs were exposed to DP at 0, 0.1, 1, 2, 5, 10, 20, 30, 40, 50, 100, and 200 μM for 3, 5, and 7 days. The activities of caspase 8 and caspase 3 (Medical & Biological Laboratories Co., Ltd., Nagoya) and the concentrations of interleukin (IL)-6, IL-1, and tumor necrosis factor (TNF)-α (Pharmingen, San Diego, CA, USA) were determined by ELISA kits and quantified by reading at 490 nm (MRX; Dynatech Laboratories, Chantilly, VA, USA). Each individual sample was analyzed in triplicate.

Real-time reverse transcription-polymerase chain reaction (RT-PCR)

For real-time RT-PCR, the total RNA was extracted using the RNAeasy kit (Qiagen, Valencia, CA, USA) as previously described (23). Briefly, total RNA (1 μg) of each sample was reversely transcribed in 20 μL using 0.5 μg of oligo dT and 200 U Superscript II RT (Invitrogen, Carlsbad, CA, USA). The amplification was carried out in a total volume of 20 μL containing 0.5 μM of each primer, 4 mM $MgCl_2$, 2 μL LightCycler™ FastStart DNA Master SYBR green I (Roche Molecular Systems, Alameda, CA, USA), and 2 μL of 1:10 diluted cDNA. The quantification in the unknown samples was performed by the LightCycler Relative Quantification Software version 3.3 (Roche Molecular Systems). In each experiment, the glyceraldehyde 3-phosphate dehydrogenase (GAPDH) housekeeping gene was amplified as a reference standard. GAPDH primers were GAPDH(f): GGGCCAAAAGGGTCATCATC (nt 414 – 434, GenBank accession no. BC059110.1); GAPDH(r): ATGACCTTGCCCACAGCCTT (nt 713 – 733). Other target gene primers were Bcl-2(f): GGGAT GACTTCTCTCGTCGCTAC (nt 527 – 550, GenBank accession no. NM_016993.1); Bcl-2(r): GTTGTCCAC CAGGGGTGACAT (nt 721 – 742); Bax(f): GTGGT TGCCCTCTTCTACTTTGC (nt 328 – 351, GenBank accession no. NM_017059.1); Bax(r): GAGGACTC CAGCCACAAAGATG (nt 522 – 544); Nestin(f): TGG AGCGGGAGTTAGAGGCT (nt 525 – 545, GenBank accession no. NM_012987.1); Nestin(r): ACCTCTAAG CGACACTCCCGA (nt 784 – 805). Reactions were prepared in duplicate and heated to 95°C for 10 min, followed by 40 cycles of denaturation at 95°C for 10 s, annealing at 55°C for 5 s, and extension at 72°C for 20 s. All PCR reactions were performed in duplicate. Standard curves (cycle threshold values versus template concentration) were prepared for each target gene and for the endogenous reference (GAPDH) in each sample. To confirm the specificity of the PCR reaction, PCR products were electrophoresed on a 1.2% agarose gel.

Immunoblot analysis

After the treatment with DP, the cell lysates of the NSCs were collected and the concentration of protein was determined by using the Bio-Rad Protein Assay kit (Bio-Rad, Hercules, CA, USA). Cell extracts with sample buffer were boiled for 5 min and then separated by a 10% SDS-PAGE gel. After electrophoresis, the gel was transferred onto a PVDF membrane for immunoblotting. The membrane was first blocked by incubation in non-fat milk at room temperature for 2 h, incubated with anti-Bcl-2 antibody (Upstate Biotechnology, Inc., Waltham, MA, USA) and anti-β actin (Chemicon International Inc., Temecula, CA, USA) for 2 h at room temperature, washed five times with Tris-buffered saline Tween-20 (TBST), and then incubated further at room temperature with horseradish peroxidase-conjugated secondary antibody for 2 h. Then the membrane was washed six times with TBST and specific bands were made visible by chemiluminescence (Santa Cruz Biotechnology, Santa Cruz, CA, USA).

Bcl-2 RNA interference

Bcl-2 double-stranded siRNA was chemically synthesized by Ambion, Inc., Austin, TX, USA. The sense and antisense sequences were designed as follows: Sense: GCGCUGGAUAUAACUUCUUtt; Antisense: AAG AAGUUAUAUCCAGCGCtt, starting from nucleotide 137 of Bcl-2 sequence (accession number L14680). In this study, the siRNA control used was siRNA-Cy3 (Qiagen), sense sequence: UUCUCCGAACGUGUCA CGUdTdT 3'-Cy3 and the complement 5'-ACGUGA CACGUUCGGAGAAdTdT 3'-Cy3) as an irrelevant control. The transfection of siRNA was performed using Lipofectamine 2000 (Invitrogen) according to the manufacturer's instructions. In brief, cells were harvested with 0.25% trypsin, 1 mM ethylenediaminetetraacetic acid (EDTA) in phosphate-buffered saline (PBS) without Ca^{2+} and Mg^{2+}, and they were plated in six-well plates at 10^5 per cm^2. Then 3.5 μl siRNA (100 μM solution) was mixed with 125 μL serum-free culture medium for 5 min at room temperature. During this incubation period, 5 μL of Lipofectamine 2000 was diluted in 125 μL serum-free culture medium. These two mixtures were combined, mixed gently, and incubated for 20 min at room temperature for complex formation. This 250 μL of siRNA-Lipofectamine mixture was then added to 2.25 mL of cells. The transfected cells were cultured and fed daily with fresh medium until they were assayed.

ELISA and terminal dUTP nick-end labeling (TUNEL) assay

The activities of caspase 8 and caspase 3 were determined by an ELISA kit (Medical & Biological Laboratories Co., Ltd.) and quantified by reading at 490 nm (MRX, Dynatech Laboratories). Each individual sample was analyzed in triplicate. Furthermore, apoptotic cells were identified by the TUNEL method (In Situ Cell Death Detection Kit, POD; Roche Boehringer Mannheim Corp., Indianapolis, IN, USA) as described by Chiou et al. (24). Briefly, the cells with coverslips were washed with 1X PBS, fixed with 4% paraformaldehyde for 10 min, permeabilized with 0.1% triton X-100 for 5 min, and incubated with the provided TUNEL reagent for 1 h. Chromogenic development was then applied with 3-amino-9-ethyl-carbazole and the slides were counterstained with H & E stain. The percentage of TUNEL-positive cells was measured by calculating the average of six different areas and comparing it to the total number of cells in the same section of the slide.

Immunofluorescence staining

An avidin-biotin complex method was used for the immunohistochemical staining in the differentiated NSCs (24). Following washes with 3% hydrogen peroxide, sodium azide and antigenicities were retrieved using a microwave. Each slide was then treated with antibody GFAP (Chemicon, Temecula, CA, USA) and MAP-2 (Chemicon). Immunoreactive signals were detected with a mixture of biotinylated rabbit anti-mouse IgG and Fluoesave (Calbiochem, La Jolla, CA, USA) under confocal microscopy (FluoView FV300; Olympus, Tokyo).

Microdialysis and HPLC-ECD

A microdialysis sampling technique system connected to the Petri dish was constructed in our own laboratory according to the design originally described by Cheng et al. (25). The dialysis probe was made of a dialysis membrane, 30 mm in length, with an outer diameter of 150 μm and a nominal molecular weight cut-off of 13000. Ringer solution (8.6 g/L NaCl, 0.3 g/L KCl, and 0.33 g/L $CaCl_2$) was perfused through the probe at a flow-rate of 2 μL/min. Microdialysate samples were collected every 10 min. An HPLC-ECD system (HTEC-500; Eicom, Kyoto) consisting of a three-electrode cell (an Ag/AgCl reference electrode, a counter electrode, and a graphite working electrode) was used to measure dopamine (DA) and determine the levels of serotonin (5-HT) and noradrenaline (NE). The graphite working electrode had a 25-μm gasket and the applied potential was set at +450 mV *vs* Ag/AgCl. The column used for separation at room temperature (25°C) was a PP-ODS (4.6 × 30 mm) (Eicom). The mobile phase, containing 0.1 M sodium phosphate buffer (0.1 M NaH_2PO_4:0.1 M Na_2HPO_4 = 1000:160, v/v), 1% methanol, 500 mg/L sodium sulfonate, and 50 mg/L EDTA, was adjusted to pH 6.0 with 5 M of NaOH and had a flow rate of 0.5 mL/min. A volume of 10 μL of each microdialysate was injected manually into the chromatographic system and assayed on the same sampling day. A sample collected from DP-treated NSC medium yielded the following peaks: 3,4-dihydroxyphenylacetic acid (DOPAC) (5.23 min), DA (6.87 min), 5-hydroxyindoleacetic acid (5-HIAA) (7.78 min), 4-hydroxy-3-methoxyphenylacetic acid (HVA) (10.90 min), and 5-HT (15.67 min). The analysis was completed within 20 min.

Statistical analyses

The results were reported as the mean ± S.E.M. Statistical analysis was performed by using the one-way or two-way ANOVA test followed by Tukey's test or Student's *t*-test, as appropriate. A P value <0.05 was considered to be statistically significant.

Results

DP modulates the cell viability of NSCs

Tissues from the hippocampus region of adult SD rats were dissociated and cultured in the DMEM/F-12 serum-free medium with EGF and bFGF (16). After being cultured for 1 week, NSCs aggregated and formed spheroid-like bodies called neurospheres (Fig. 1A). To investigate the neuron-lineage differentiation, the neurospheres were further cultured in the induction medium with 2% fetal bovine serum (FBS) for 14 days and then gradually differentiated into neural-like cells (Fig. 1: B, C, and D). By using the immunofluorescent assay, the percentages of GFAP-positive cell were 38.7 ± 6.1% (GFAP: astroglia marker; red color; Fig. 1C) and the percentages of MAP-2-positive neurons were 33.4 ± 5.3% (MAP-2: mature neuron marker; green color; Fig. 1D) and were detected in the differentiated NSCs. Furthermore, the cell viability and proliferation of NSCs were analyzed by using the MTT assay. NSCs were exposed to 0, 0.1, 1, 2, 5, 10, 20, 30, 40, 50, 100, and 200 μM of DP for 3, 5, and 7 days (Fig. 2A). Our data showed that the cell proliferation was significantly increased in 2 μM DP-treated NSCs at Day 3, Day 5 and Day 7 cultures (Fig. 2: A and B; P<0.05). Since DP at 2 μM was shown to effectively increase cell survival (Fig. 2), the concentration of 2 μM DP was chosen for all further experiments.

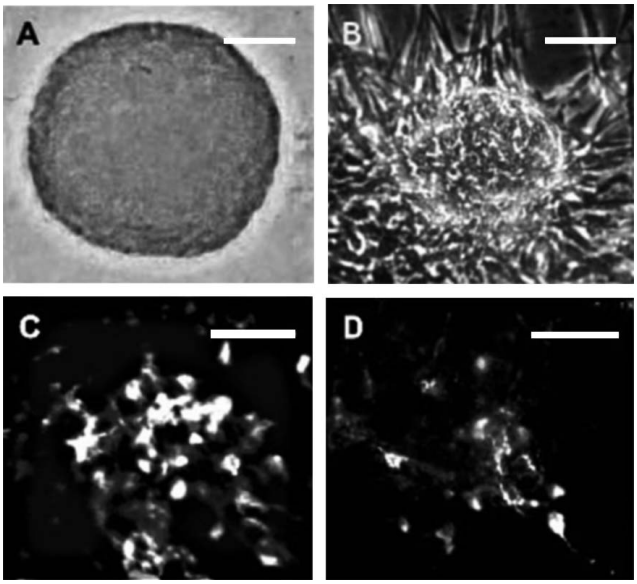

Fig. 1. Isolation and cultivation of neural stem cells (NSCs) from the hippocampal region of adult Sprague-Dawley rats. A: NSCs aggregated and formed neurospheres in serum-free medium culture. B, C, and D: After addition of 2% fetal bovine serum, the neurospheres then attached to the culture plate and gradually differentiated into neural-like cells. The GFAP-positive cells (red fluorescent) (C) and the MAP-2 positive (green fluorescent) neurons (D) were detected in the differentiated NSCs. A – D were performed in three separate experiments, Bar: 30 μm.

Detection of Bcl-2 expression in DP-treated NSCs by real-time RT-PCR and Western blotting

To further investigate whether the anti-apoptosis (Bcl-2), apoptosis (Bax and Bad), and neuron-lineage differentiation (MAP2 and nestin) play critical roles in the molecular mechanisms of the differentiation process in DP-treated NSCs, mRNA expressions of Bcl-2, Bax, Bad, MAP-2 (mature neuron marker), and nestin (neural progenitor marker) were detected in Day 3, 5, and 7 samples. By using the real time RT-PCR method, the results showed that mRNA levels of Bcl-2 and nestin in Day 5 and 7 DP (2 μM)-treated NSCs were significantly increased when compared to non-DP-treated NSCs (P<0.05, Fig. 3A). However, the expressions of Bax and Bad were not activated in Day 3, 5, and 7 DP-treated NSCs (Fig. 3A). Furthermore, when compared to Day 7 non-DP-treated NSCs, the levels of Bcl-2 mRNA were significantly increased in the 0.1, 1, 2, and 5 μM DP-treated, Day 7 NSC groups in a dose-dependent manner (Fig. 3B). By using the Western blot method, the Bcl-2 protein expression in Day 3 DP-treated NSCs was higher than that in Day 3 non-DP-treated NSCs (as a control, P<0.05; Fig. 4: A and B). The Bcl-2 expression level in Day 7 DP-treated NSCs was significantly inhibited by the transfection of Bcl-2 siRNA (Fig. 4: A and B). Moreover, the protein expression level of Bcl-2 was significantly increased in DP- and LPS-treated NSCs (Fig. 4C), and it was also effectively inhibited by the treatment of Bcl-2 siRNA (Fig. 4C).

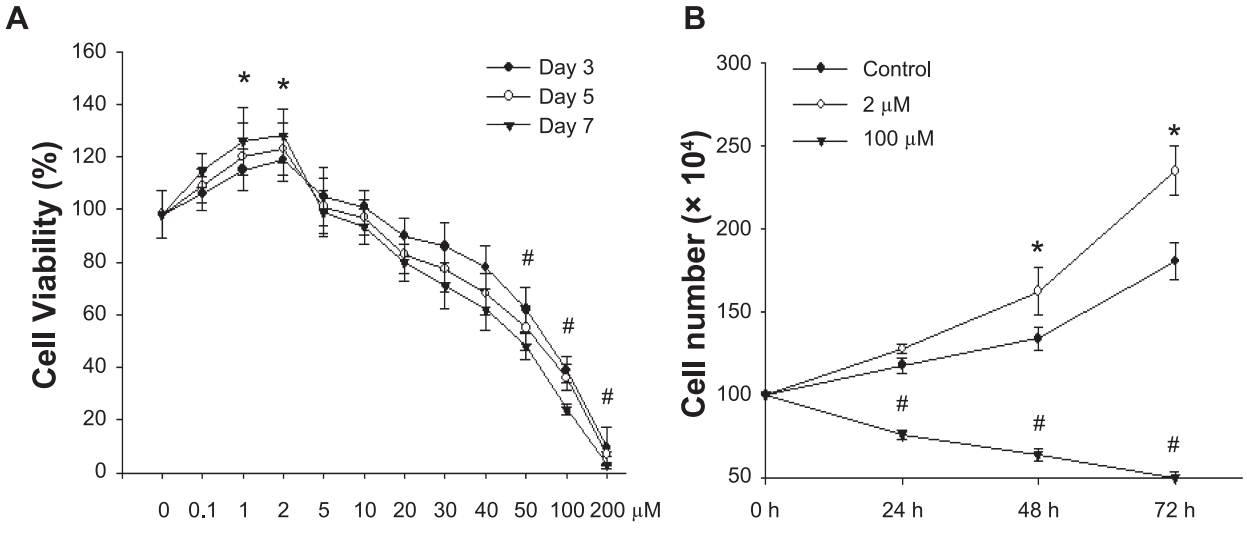

Fig. 2. Evaluation of neural stem cell (NSC) proliferation and viability in different desipramine (DP)-treated concentrations by methyl thiazol tetrazolium assay. A: NSCs were cultured in the presesnce of 0, 0.1, 1, 2, 5, 10, 20, 30, 40, 50, 100, and 200 μM DP for 3, 5, and 7. B: Cell numbers of DP-treated NSCs after 24, 48, and 72 h were counted by a hemocytometer: 10^4 NSCs were plated on 6-cm culture dishes with or without DP. After treating with DP for 72 h, cell numbers were significantly increased in 2 μM DP-treated NSCs but significantly decreased in 100 μM DP-treated NSCs. Data (mean ± S.E.M. of six separate experiments) are expressed as percentages of the control value (non-DP-treated). *P<0.05, compared to the control; $^{\#}P$<0.05, compared to the control. The vehicle control used was 0.1% dimethyl sulfoxide.

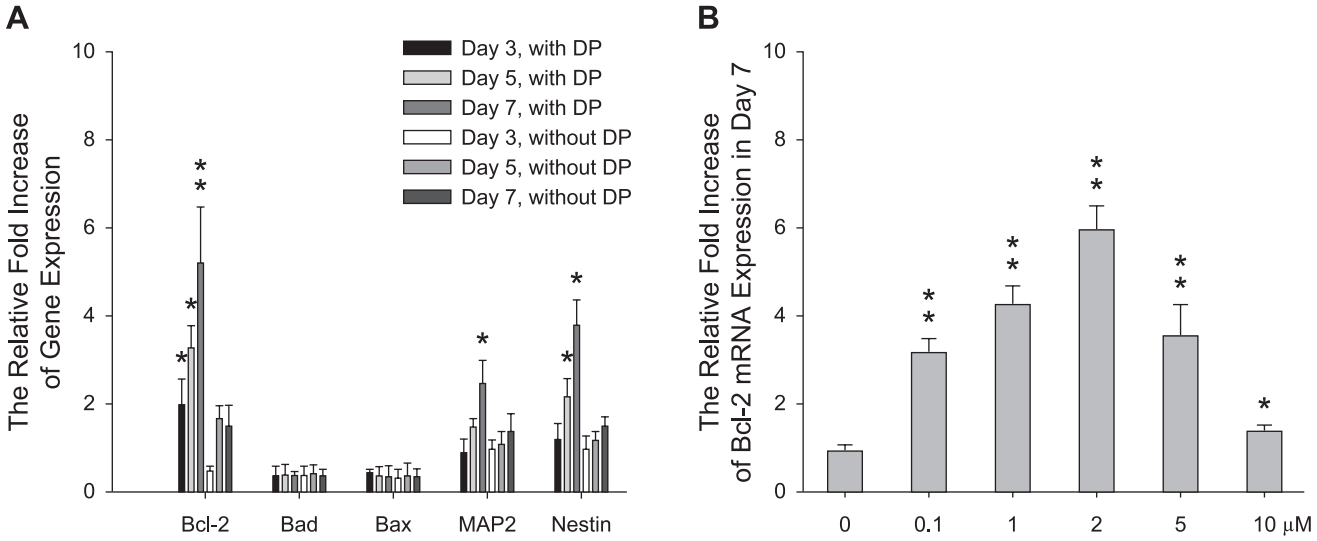

Fig. 3. Detection of mRNA expressions in desipramine (DP)-treated neural stem cells (NSCs) by the real time reverse transcriptase polymerase chain reaction (RT-PCR). A: By using the real-time RT-PCR method, the mRNA expression levels of Bcl-2, Bad, Bax, MAP-2, and nestin genes were measured in DP-treated and non-D-treated NSCs on the different culture days (Day 3, 5, and 7). Data shown here are each the mean ± S.E.M. of three experiments. **P*<0.05, ***P*<0.01, DP-treated NSCs as compared to non-DP-treated NSCs on the same days. B: The mRNA expression levels of Bcl-2 in NSCs treated with different concentrations of DP in Day 7 culture. Data shown here are each the mean ± S.E.M. of three experiments; **P*<0.05, ***P*<0.01, compared to Day 7 non-DP-treated NSCs.

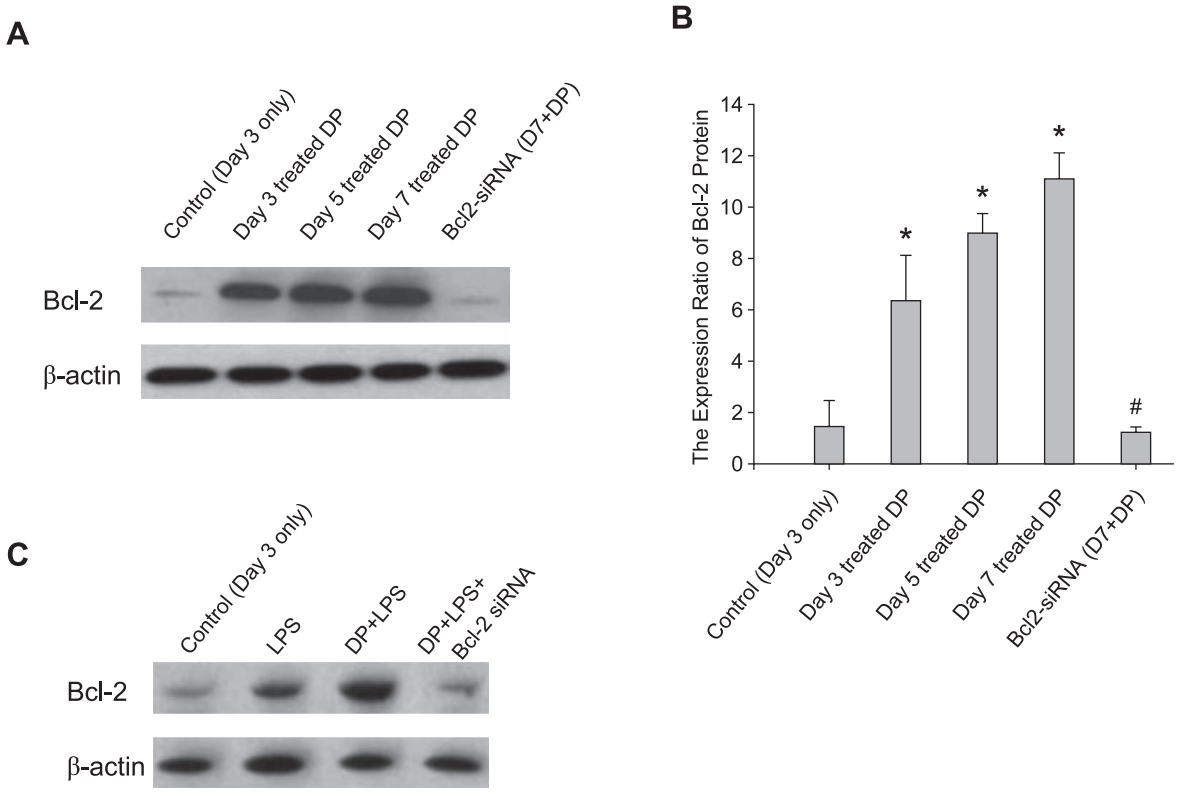

Fig. 4. Detection of Bcl-2 expression by Western blotting in desipramine (DP)-treated neural stem cells (NSCs). A: Detection of Bcl-2 protein expression in Day 3, 5, and 7 DP-treated NSCs; Control: Day 3 non-DP-treated NSCs. The Bcl-2 level in Day 7 DP-treated NSCs was significantly inhibited by the transfection of Bcl-2 siRNA (D7 + DP). B: Bcl-2 protein expression level in Day 3 DP-treated NSCs was higher than that in Day 3 non-DP-treated NSCs. Data shown here are each the mean ± S.E.M. of three experiments. **P*<0.05, *vs* Control; #*P*<0.05, *vs* Day 7 DP-treated NSCs. C: Detection of Bcl-2 protein expression in NSCs treated with LPS only, DP + LPS, and DP + LPS + Bcl-2 siRNA after 3 days culture; Control: Day 3 NSCs without any treatment.

DP treatment protects against LPS-induced apoptosis and inhibits LPS-induced proinflammatory effects in NSCs

LPS is a highly proinflammatory component of the outer member of gram-negative bacteria and has been tested as a stress model for inducing caspase-dependent apoptosis (26, 27). We further investigated whether the up-regulation of Bcl-2 induced by 2 μM DP could inhibit the LPS-induced apoptosis in DP-treated NSCs. Under LPS (100 ng/mL) exposure, we found that the apoptotic activities of caspase 8 and caspase 3 in Day 3, 5, and 7 DP-treated NSCs groups were significantly decreased when compared to those in the non-DP-treated NSCs group (P<0.05, Fig. 5: A and B). Consistent with the caspase 8 and caspase 3 data, the results of TUNEL assay further confirmed that DP treatment could protect against LPS-induced apoptosis in the DP-treated NSCs (Fig. 5C) but not in the non-DP-treated NSCs group (Fig. 5: A, B, and C). Our result also revealed that 40 μM of the pan-caspase inhibitor Z-VAD-fmk prevented

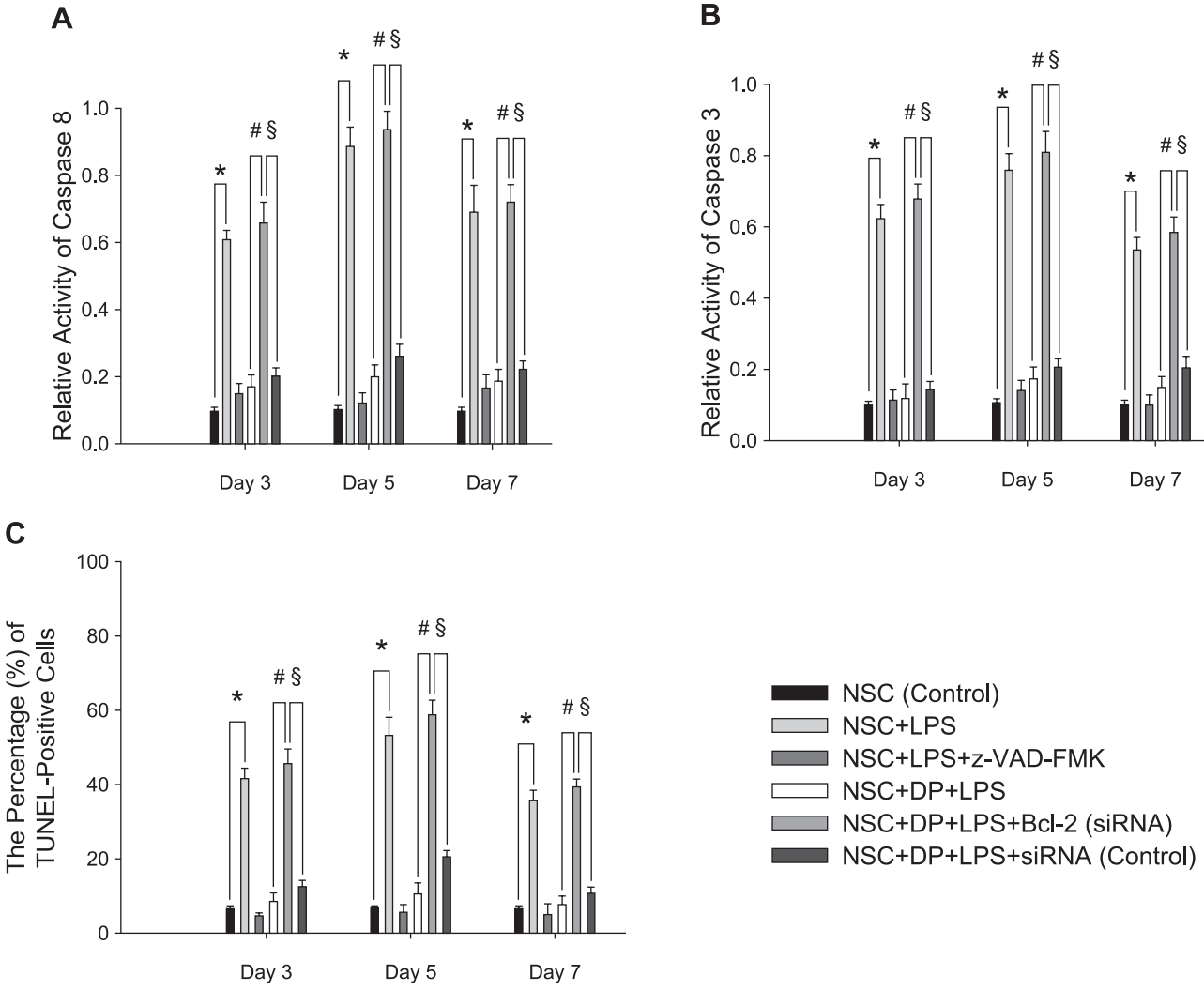

Fig. 5. Evaluation of lipopolysaccharide (LPS)-induced apoptotic activity of caspase 8 and caspase 3 in desipramine (DP)-pretreated and non-DP-pretreated neural stem cells (NSCs) by ELISA test and TUNEL assay. To investigate the neuroprotection ability of DP treatment in LPS-treated NSCs, the apoptotic activities of caspase 8 (A) and caspase 3 (B) induced by LPS in DP- or non-DP-pretreated NSCs were evaluated by ELISA assay; the ratio of non-DP treated NSCs was defined as 0.1, and the relative activities of caspase 8 and 3 in the differently treated groups were compared to non-DP treated NSCs. C: The severity of DNA fragmentation induced by LPS in DP- and non-DP-pretreated NSCs was analyzed by TUNEL assay; the ratio of non-DP-treated NSCs was defined as 0.1 and the relative apoptotic activity in the differently treated groups was compared to non-DP treated NSCs. Control: medium only, NSC + LPS: NSCs treated with LPS at 100 ng/mL, Z-VAD-FMK (a pan-caspase inhibitor, 40 μM). Data shown here are each the mean ± S.E.M. of three experiments. *P<0.05, control group *vs* NSC + LPS; $^{\#}P$<0.05, NSC + DP + LPS *vs* NSC + DP + LPS + Bcl-2 siRNA; $^{\S}P$<0.05, NSC + DP + LPS + Bcl-2 siRNA *vs* NSC + DP + LPS + siRNA (control).

LPS-induced apoptosis in NSCs through the inhibition of the activities of caspase 8, caspase 3, and DNA fragmentation (Fig. 5: A, B, and C). Moreover, by using siRNA inhibition of Bcl-2, the activities of LPS-induced apoptosis were significantly elevated when combined with LPS- and DP-treated NSCs (Fig. 5: A, B, and C). This result confirmed that DP prevents LPS-inducing caspase-dependent apoptosis in NSCs through the activation of Bcl-2.

Furthermore, to investigate the anti-inflammatory effects of DP in NSCs, the LPS-induced model was used and the levels of IL-1β, IL-6, and TNF-α were examined by the ELISA test. The results showed that the levels of IL-1β, IL-6, and TNF-α in the LPS-treated NSCs were significantly increased when compared to those in the control group (NSCs only; $P<0.05$; Fig. 6: A, B, and C). Our results confirmed that DP treatment can effectively reduce IL-1β, IL-6, and TNF-α production (Fig. 6: A, B, and C). Furthermore, by using siRNA inhibition of Bcl-2 in NSCs, the levels of IL-1β, IL-6, and TNF-α were significantly elevated when combined with LPS- and DP-treated NSCs (Fig. 6: A, B, and C).

Detection of concentrations of NE, DA, and 5-HT released from DP-treated NSCs by HPLC

To further identify the functional production of NE, DA, and 5-HT in these NSC-derived neurons, the method of microdialysis coupled with HPLC-ECD was used to measure the concentration of NE, DA, and 5-HT in the medium of the DP-treated NSCs (Fig. 7). Our results showed that DP can significantly stimulate the functional releases of NE and 5-HT in the DP-treated NSCs, but not the DA production (Fig. 7: A, B, C). To investigate the possible mechanism associated with the mitogen activated protein kinase/extracellular-regulated kinase (MAPK/ERK) pathway, the MAPK inhibitor U0126 was added to the DP-treated NSCs. The results showed that the functional productions of NE, 5-HT, and even DA were significantly diminished in DP-treated NSCs after addition of U0126 treatment (Fig. 7).

Bcl-2, an anti-apoptotic protein, is the down-stream protein of ERK and can be up-regulated through activation of the MAPK/ERK pathway. To further evaluate the role of Bcl-2 in the modulation of neurotransmitter release in NSCs, the Bcl-2 siRNA was transfected into NSCs with or without DP treatment. The results showed that the production of NE and 5-HT in the DP-treated NSCs can be partially inhibited by the treatment of Bcl-

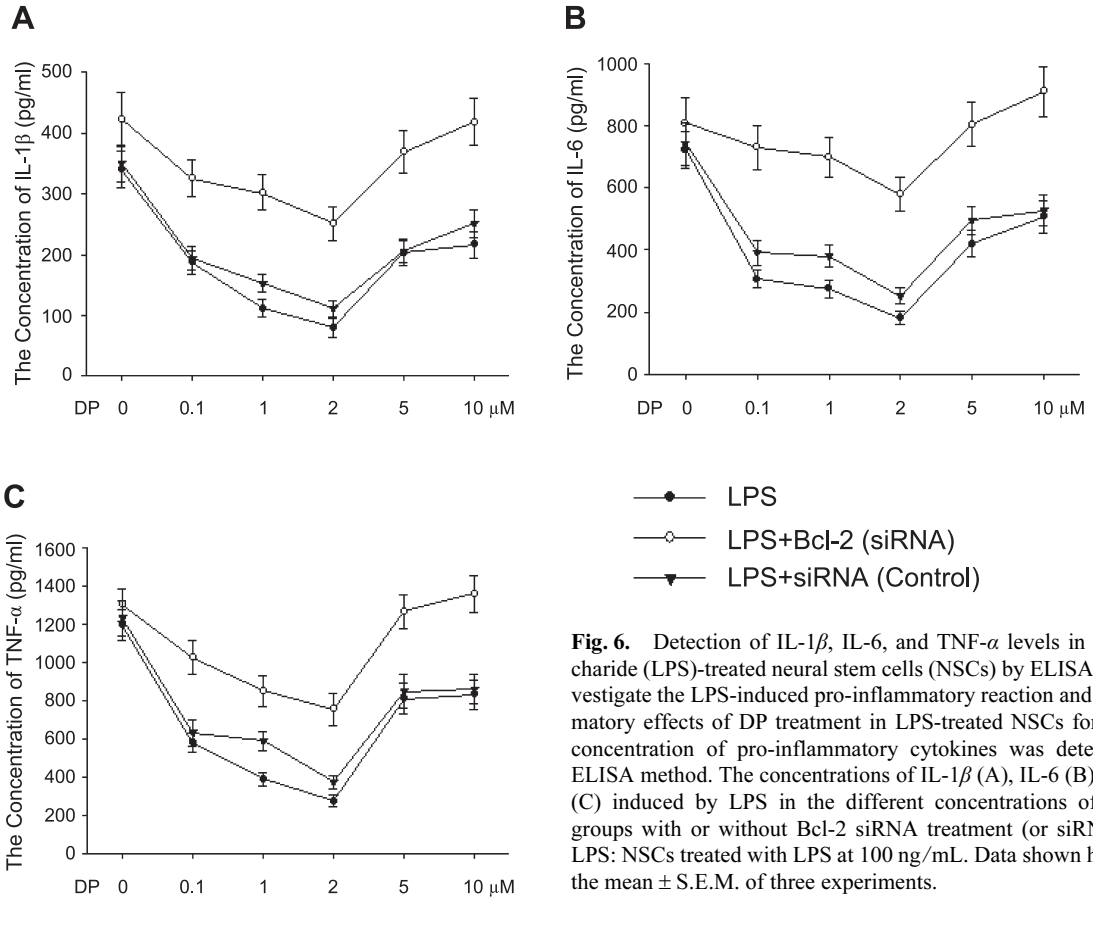

Fig. 6. Detection of IL-1β, IL-6, and TNF-α levels in lipopolysaccharide (LPS)-treated neural stem cells (NSCs) by ELISA tests. To investigate the LPS-induced pro-inflammatory reaction and anti-inflammatory effects of DP treatment in LPS-treated NSCs for 3 days, the concentration of pro-inflammatory cytokines was detected by the ELISA method. The concentrations of IL-1β (A), IL-6 (B), and TNF-α (C) induced by LPS in the different concentrations of DP-treated groups with or without Bcl-2 siRNA treatment (or siRNA control). LPS: NSCs treated with LPS at 100 ng/mL. Data shown here are each the mean ± S.E.M. of three experiments.

2 siRNA (Fig. 7: A and C). Moreover, our results showed that 5-HT levels in Day 3, Day 5, 7, and 14 DP-treated NSCs culture mediums were significantly higher than in those of non-DP-treated NSCs (P<0.05, Fig. 7D). We also found that the production of 5-HT in Day 3, 5, 7, and Day 14 DP-treated NSCs were significantly inhibited by the transfection of Bcl-2 siRNA (P<0.05, Fig. 7: C and D). In contrast to the inhibition effects of siRNA on Bcl-2, the concentrations of 5-HT in the siRNA control group were higher than those in the Bcl-2 siRNA-treated and non-DP-treated groups (P<0.05, Fig. 7: C and D).

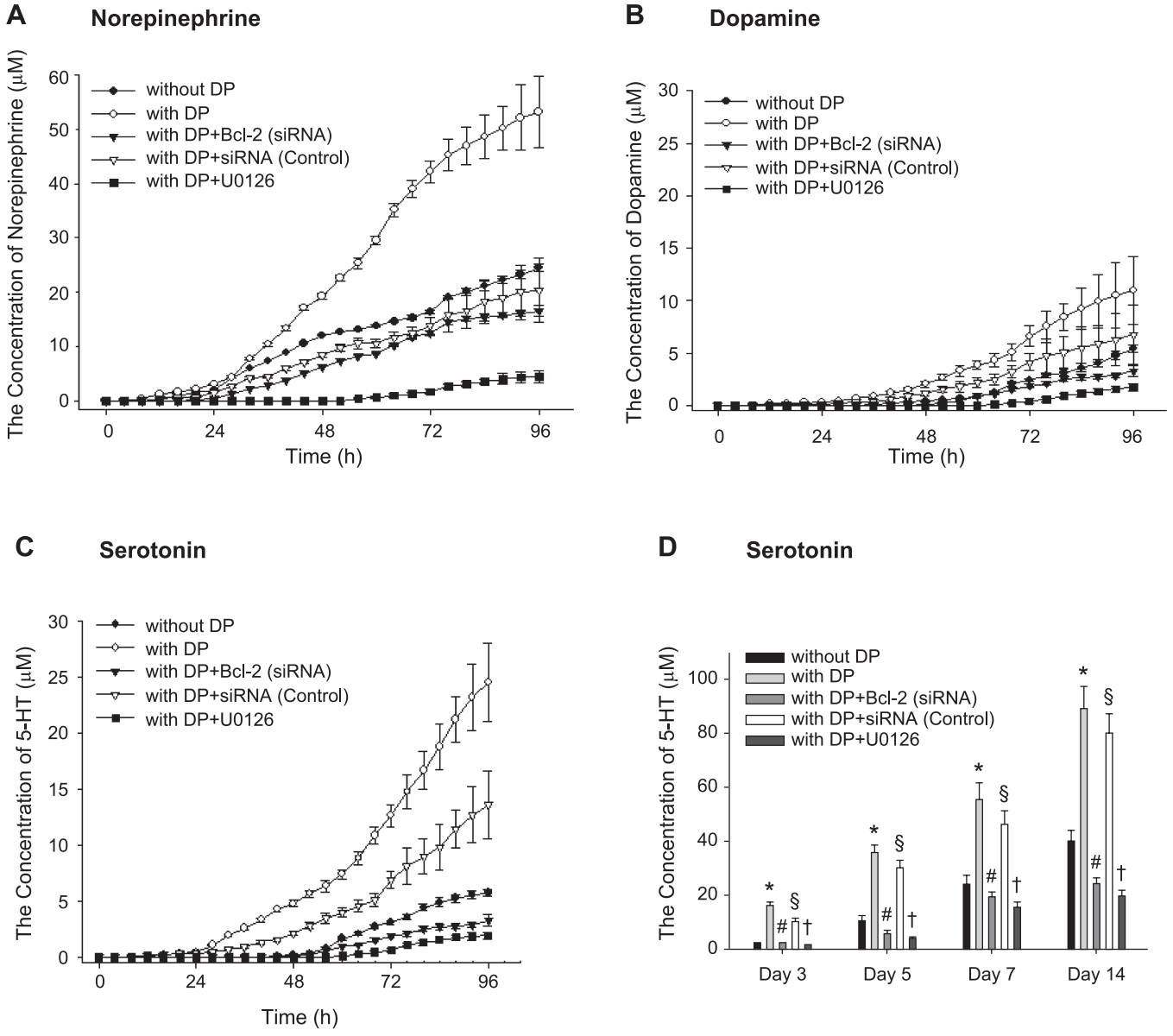

Fig. 7. Detection of norepinephrine (NE), dopamine (DA), and serotonin (5-HT) levels in the culture medium of desipramine (DP)-treated neural stem cells (NSCs) by microdialysis with HPLC-ECD. A: By using microdialysis with HPLC-ECD, the NE levels were continuously monitored in the culture medium of 24, 48, 72, and 96 h non-DP-treated NSCs (control), DP-treated NSCs, DP + Bcl-2 siRNA-treated NSCs, DP + siRNA control-treated NSCs, and DP+U0126-treated NSCs. B: Continuous monitoring of DA levels in the medium of 24, 48, 72, and 96 h NSCs with different treatments. C: Continuous monitoring of 5-HT in the medium of 24, 48, 72, and 96 h NSCs with different treatments. D: The levels of 5-HT in Day 3, 5, 7, and 14 culture medium of non-DP-treated NSCs (control), DP-treated NSCs, DP + Bcl-2 siRNA-treated NSCs, DP + siRNA control-treated NSCs, and DP + U0126-treated NSCs. Data shown here are each the mean ± S.E.M. of six experiments. *P<0.05: NSC + DP *vs* non-DP-treated (control) group; $^{\#}P$<0.05: NSC + DP + Bcl-2 siRNA *vs* NSC + DP; $^{\S}P$<0.05: NSC + DP + siRNA (control) *vs* NSC + DP + Bcl-2 siRNA. $^{\dagger}P$<0.05: NSC + DP + U0126 *vs* NSC + DP.

Discussion

The hippocampus has long been associated with learning, memory, and the modulation of emotional responses (8). Several studies have demonstrated that stress-induced atrophy and loss of hippocampal CA3 pyramidal neurons may contribute to the pathogenesis of depression (28). Recently, a novel theory for depression treatment has been proposed; that is, the regulation of neurogenesis in the adult brain is a target for the action of antidepressant drugs (29, 30). By using the in vitro culture of NSCs from the hippocampus of adult rats (Fig. 1), our study demonstrated that the 2 μM DP is the optimal concentration for increasing viability and proliferation in the different concentrations (0.1, 1, 5, 10, 20, 30, 40, 50, 100, and 200 μM) of DP-treated NSCs (Fig. 2). We found that the cell viabilities of NSCs were slightly decreased in 50 μM DP and significantly declined when the concentration of DP was beyond 100 μM (Fig. 2). The result of real-time RT-PCR further supported the view that Bcl-2 mRNA levels increased the most in 2 μM DP-treated NSCs compared to the other groups (Fig. 3B). Furthermore, using the TUNEL assay and the siRNA method, our data confirmed that 2 μM DP-treated NSCs can effectively prevent LPS-induced apoptosis and the production of proinflammatory cytokines in the NSCs through the up-regulation of Bcl-2 expression (Figs. 5 and 6). More importantly, by using Bcl-2 siRNA and continuous evaluation microdialysis coupled with HPLC-ECD, we confirmed that DP facilitates the release of 5-HT and norepinephrine from NSCs via the activation of Bcl-2 (Fig. 7).

Bcl-2, an anti-apoptotic protein, has recently been identified as a neuronal cell death repressor and plays an important role in the protection of neural cell death caused by chemical damage and hypoxia (31). Our data demonstrated that NSCs possess the multi-lineage ability of astroglia ($38.7 \pm 6.1\%$) and mature neurons ($33.4 \pm 5.3\%$, Fig. 1). The previous study showed that the subcellular distribution of Bcl-2 was similar between in vivo (brain) and in vitro (culture) conditions and between cultured neurons and astrocytes, while the content was higher in astrocytes than in neurons (32). Ozdener et al. further found that inducible functional expressions of Bcl-2 in human astrocytes play important roles in both neuroprotection and neurodegeneration (33). As for the detailed mechanisms involved in the effect of DP on differentiating NSCs, elevated Bcl-2 mRNA and protein levels were found in this study (Figs. 3 and 4). We used the method of Bcl-2 siRNA to induce sequence-specific degradation of Bcl-2 mRNA or inhibit translation of Bcl-2 complementary mRNA in the transfected NSCs. As shown in Fig. 5, the apoptotic activities (caspase 8, caspase 3, and TUNEL) were significantly increased in the DP/LPS/Bcl-2 siRNA-treated NSCs compared to the DP/LPS-treated NSCs. Our results indicated that DP increased the anti-apoptotic activity in NSCs through the modulation of Bcl-2 expression. Thus, the neuroprotective effect of DP-treated NSCs could be attributed to the activation of Bcl-2 and thereby protect against LPS-induced apoptosis in NSCs.

Recent studies have suggested that major depression is accompanied by the activation of the inflammatory-response system. It has been hypothesized that increased production of proinflammatory cytokines may play a role in the pathophysiology of depressive disorders (17 – 19). Some studies have observed a strongly positive correlation between IL-6, TNF-α, and IL-1β cytokine levels and depressive symptoms (17 – 19, 34). Furthermore, Hellstrom et al. confirmed that LPS exposure dramatically increased IL-1β- and the IL-1β-dependent IL-6 level in hippocampal slices and the culture medium of hippocampal neurons (35). In this study, we found that the levels of IL-6, TNF-α, and IL-1β induced by LPS were significantly inhibited by DP (Fig. 6: A, B, and C). Consistent with our findings, Kubera et al. demonstrated that antidepressant drugs can inhibit the release of IL-1, IL-6, and TNF-α induced by LPS (36). Moreover, by using siRNA inhibition of Bcl-2, our data confirmed that DP effectively diminishes the production of proinflammatory cytokines in DP-treated NSCs through the activation of Bcl-2 expression (Fig. 6: A, B, and C). To summarize, our data indicated that DP not only protects against NSC apoptosis but also plays a key role in the anti-inflammatory effect in depression through the activation of Bcl-2.

The MAPK/ERK signaling pathways have been noted for transcriptional activation and protein synthesis of neuronal survival and neuroplasticity in depression (37 – 39). Importantly, Duman et al. recently demonstrate that acute blockade of MAPK signaling produces a depressive-like phenotype and blocks behavioral actions of antidepressants (40). Moreover, the activation of the MAPK/ERK pathway can inhibit apoptosis by inducing the phosphorylation of Bad (a pro-apoptotic protein) and increasing the expression of Bcl-2 (39, 41). Bcl-2 is also a target for the actions of mood stabilizers, mediates many of the beneficial effects of endogenous neurotrophic factors, and enhances cellular resilience in the treatment of mood disorders (21, 22, 42). Jiao et al. further demonstrated that Bcl-2 enhanced endoplasmic reticulum calcium signaling through ERK phosphorylation to support the intrinsic regenerative capacity of CNS axons (43). By using the real-time and continuous evaluation of microdialysis coupled with HPLC-ECD,

our results showed that DP can significantly stimulate the functional releases of NE and 5-HT in DP-treated NSCs but not DA production (Fig. 7). Furthermore, the production of NE and 5-HT in DP-treated NSCs can be partially inhibited by the treatment of Bcl-2 siRNA (Fig. 7). To further explore the role of the MAPK/ERK pathway (up-stream cellular signaling of Bcl-2 associated with DP treatment), the MAPK inhibitor U0126 was used. The results showed that the functional productions of NE, 5-HT, and even DA were significantly diminished in DP-treated NSCs after addition of U0126 (Fig. 7). Indeed, our findings supported the view that the MAPK/ERK pathway plays a critical role in the regulation of functional release of neurotransmitters in antidepressant treatment.

Neurotransmitters, like 5-HT and NE, play an important role in neurogenic effects, immune modulation, and synaptic plasticity in the adult CNS (44). Ou et al. reported that monoamine oxidase A can degrade 5-HT, NE, and DA and is involved in apoptotic signaling pathway mediated by caspase 3 (45). Antidepressant drugs may further increase the production of 5-HT and promote the abilities of neuroprotection in neural progenitor cells through Bcl-2 and Bcl-xL activation (45, 46). In agreement with these findings, we firstly demonstrated that DP treatment cannot only work against the LPS-induced apoptosis but also effectively block the LPS-induced pro-inflammatory reaction in DP-treated NSCs mediated by Bcl-2 activation. Thus, in addition to the current understanding concerning the mechanism of DP, in vitro culture of NSCs indeed provides an effective system to elucidate the underlying mechanisms of neurogenesis and neuroprotection. Moreover, this in vitro model of NSCs could be considered a valuable tool for discovering new mechanisms of antidepressant drugs and in screening the candidate agents for the treatment of neurodegenerative diseases.

Acknowledgments

This study was supported by research grants from the TVGH (95/96-C1-150), the Joint Projects of UTVGH (95/96-P1-08), Yen-Tjing-Ling Medical Foundation, and National Yang-Ming University (Ministry of Education, Aim for the Top University Plan), Taiwan.

References

1 Friedman RA, Kocsis JH. Pharmacotherapy for chronic depression. Psychiatr Clin North Am. 1996;19:121–132.
2 Cipriani A, Brambilla P, Furukawa T, Geddes J, Gregis M, Hotopf M, et al. Fluoxetine versus other types of pharmacotherapy for depression. Cochrane Database Syst Rev. 2005;4: CD004185.
3 Martinez TR, Frechilla D, Del RJ. Chronic antidepressant treatment increases the membrane expression of AMPA receptors in rat hippocampus. Neuropharmacology. 2002;43: 1230–1237.
4 Carignani C, Corsi M. Inhibition of SK3 channels in the TE671 human medulloblastoma cell line by desipramine and imipramine. Eur J Pharmacol. 2002;448:139–142.
5 Pariante CM, Makoff A, Lovestone S, Feroli S, Heyden A, Miller AH, et al. Antidepressants enhance glucocorticoid receptor function in vitro by modulating the membrane steroid transporters. Br J Pharmacol. 2001;134:1335–1343.
6 Shin JG, Park JY, Kim MJ, Shon JH, Yoon YR, Cha IJ, et al. Inhibitory effects of tricyclic antidepressants (TCAs) on human cytochrome P450 enzymes in vitro: Mechanism of drug interaction between TCAs and phenytoin. Drug Metab Dispos. 2002;30:1102–1107.
7 Morishita S, Watanabe S. Effect of the tricyclic antidepressant desipramine on protein kinase C in rat brain and rabbit platelets in vitro. Psychiatry Clin Neurosci. 1997;51:249–252.
8 Sapolsky RM. Why stress is bad for your brain. Science. 1996;273:749–750.
9 Gurvits TV, Shenton ME, Hokama H, Ohta H, Lasko NB, Gilbertson MW, et al. Magnetic resonance imaging study of hippocampal volume in chronic, combat-related posttraumatic stress disorder. Biol Psychiatry. 1996;40:1091–1099.
10 Lee HJ, Kim JW, Yim SV, Kim MJ, Kim SA, Kim YJ, et al. Fluoxetine enhances cell proliferation and prevents apoptosis in dentate gyrus of maternally separated rats. Mol Psychiatry. 2001;610:725–728.
11 Santarelli L, Saxe M, Gross C, Surget A, Battaglia F, Dulawa S, et al. Requirement of hippocampal neurogenesis for the behavioral effects of antidepressants. Science. 2003;301:805–809.
12 Chen H, Pandey GN, Dwivedi Y. Hippocampal cell proliferation regulation by repeated stress and antidepressants. Neuroreport. 2006;17:863–867.
13 Gage FH. Mammalian neural stem cells. Science. 2000;287: 1433–1438.
14 Goldman S. Stem and progenitor cell-based therapy of the human central nervous system. Nat Biotechnol. 2005;23:862–871.
15 Yasuki I. Control of proliferation and differentiation of neural precursor cells: focusing on the developing cerebellum. J Pharmacol Sci. 2006;101:183–188.
16 Liu IH, Chen SJ, Ku HH, Kao CL, Tsai FT, Hsu WM, et al. Comparison of the proliferation and differentiation ability between adult rat retinal stem cells and cerebral cortex-derived neural stem cells. Ophthalmologica. 2005;219:171–176.
17 Maes M. The immunoregulatory effects of antidepressants. Hum Psychopharmacol. 2001;16:95–103.
18 Penninx BW, Kritchevsky SB, Yaffe K, Newman AB, Simonsick EM, Rubin S, et al. Inflammatory markers and depressed mood in older persons: results from the Health, Aging and Body Composition study. Biol Psychiatry. 2003;54:566–572.
19 O'Brien SM, Scott LV, Dinan TG. Cytokines: abnormalities in major depression and implications for pharmacological treatment. Hum Psychopharmacol. 2004;19:397–403.

20 Reichenberg A, Yirmiya R, Schuld A, Kraus T, Haack M, Morag A, et al. Cytokine-associated emotional and cognitive disturbances in humans. Arch Gen Psychiatry. 2001;58:445–452.
21 Manji HK, Moore GJ, Rajkowska G, Chen G. Neuroplasticity and cellular resilience in mood disorders. Mol Psychiatry. 2000;5:578–593.
22 Bachmann RF, Schloesser RJ, Gould TD, Manji HK. Mood stabilizers target cellular plasticity and resilience cascades: mplications for the development of novel therapeutics. Mol Neurobiol. 2005;32:173–202.
23 Kao CL, Chiou SH, Chen YJ, Singh S, Lin HT, Liu RS, et al. Increased expression of osteopontin gene in atypical teratoid /rhabdoid tumor of the central nervous system. Mod Pathol. 2005;18:769–778.
24 Chiou SH, Liu JH, Hsu WM, Chen SS, Chang SY, Juan LJ, et al. Up-regulation of Fas ligand expression by human cytomegalovirus immediate-early gene product 2: a novel mechanism in cytomegalovirus-induced apoptosis in human retina. J Immunol. 2001;167:4098–4103.
25 Cheng FC, Kuo JS, Huang HM, Yang DY, Wu TF, Tsai TH. Determination of catecholamines in pheochromocytoma cell (PC-12) culture medium by microdialysis-microbore liquid chromatography. J Chromatogr A. 2000;870:405–411.
26 Franchi L, Condo I, Tomassini B, Nicolo C, Testi R. A caspase-like activity is triggered by LPS and is required for survival of human dendritic cells. Blood. 2003;102:2910–2915.
27 Yu LC, Flynn AN, Turner JR, Buret AG. SGLT-1-mediated glucose uptake protects intestinal epithelial cells against LPS-induced apoptosis and barrier defects: a novel cellular rescue mechanism? FASEB J. 2005;19:1822–1835.
28 McEwen BS. The neurobiology of stress: from serendipity to clinical relevance. Brain Res. 2000;886:172–189.
29 Wright SC, Zhong J, Larrick JW. Inhibition of apoptosis as a mechanism of tumor promotion. FASEB J. 1994;8:654–660.
30 Kodama M, Fujioka T, Duman RS. Chronic olanzapine or fluoxetine administration increases cell proliferation in hippocampus and prefrontal cortex of adult rat. Biol Psychiatry. 2004;56:570–580.
31 Myers KM, Fiskum G., Liu Y, Simmens SJ, Bredesen DE, Murphy AN. Bcl-2 protects neural cells from cyanide/aglycemia-induced lipid oxidation, mitochondrial injury, and loss of viability. J Neurochem. 1995;65:2432–2440.
32 Mizuguchi M, Ikeda K, Asada M, Mizutani S, Kamoshita S. Expression of Bcl-2 protein in murine neural cells in culture. Brain Res. 1994;649:197–202.
33 Ozdener H. Inducible functional expression of Bcl-2 in human astrocytes derived from NTera-2 cells. J Neurosci Methods. 2007;159:8–18.
34 Thomas AJ, Davis S, Morris C, Jackson E, Harrison R, O'Brien JT. Increase in interleukin-1beta in late-life depression. Am J Psychiatry. 2005;162:175–177.
35 Hellstrom IC, Danik M, Luheshi GN, Williams S. Chronic LPS exposure produces changes in intrinsic membrane properties and a sustained IL-beta-dependent increase in GABAergic inhibition in hippocampal CA1 pyramidal neurons. Hippocampus. 2005; 15:656–664.
36 Kubera M, Lin AH, Kenis G., Bosmans E, van Bockstaele D, Maes M. Anti-inflammatory effects of antidepressants through suppression of the interferon-gamma/interleukin-10 production ratio. J Clin Psychopharmacol. 2001;21:199–206.
37 Einat H, Yuan P, Gould TD, Li J, Du J, Zhang L, et al. The role of the extracellular signal-regulated kinase signaling pathway in mood modulation. J Neurosci. 2003;23:7311–7316.
38 Mercier G, Lennon AM, Renouf B, Dessouroux A, Ramauge M, Courtin F, et al. MAP kinase activation by fluoxetine and its relation to gene expression in cultured rat astrocytes. J Mol Neurosci. 2004;24:207–216.
39 Hayley S, Poulter MO, Merali Z, Anisman H. The pathogenesis of clinical depression: stressor- and cytokine-induced alterations of neuroplasticity. Neuroscience. 2005;135:659–678.
40 Duman CH, Schlesinger L, Kodama M, Russell DS, Duman RS. A role for MAP kinase signaling in behavioral models of depression and antidepressant treatment. Biol Psychiatry. 2007;61: 661–670.
41 Choi IJ, Kim JS, Kim JM, Jung HC, Song IS. Effect of inhibition of extracellular signal-regulated kinase 1 and 2 pathway on apoptosis and bcl-2 expression in Helicobacter pylori-infected AGS cells. Infect Immun. 2003;71:830–837.
42 Segal RA, Greenberg ME. Intracellular signaling pathways activated by neurotrophic factors. Annu Rev Neurosci. 1996;19: 463–489.
43 Jiao J, Huang X, Feit-Leithman RA, Neve RL, Snider W, Dartt DA, et al. Bcl-2 enhances Ca(2+) signaling to support the intrinsic regenerative capacity of CNS axons. EMBO J. 2005; 24:1068–1078.
44 Lesch KP. Serotonergic gene expression and depression: implications for developing novel antidepressants. J Affect Disord. 2001;62:57–76.
45 Ou XM, Chen K, Shih JC. Monoamine oxidase A and repressor R1 are involved in apoptotic signaling pathway. Proc Natl Acad Sci U S A. 2006;103:10923–10928.
46 Egan CG. Differentiation of hippocampal stem cells into functional neurons: evolving our understanding of monoamine oxidase-A inhibition. Br J Pharmacol. 2006;148:563–564.